

Fabrication, Thermal Stability and Mechanical Properties of Porous Bulk Glassy Pd-Cu-Ni-P Alloys

Takeshi Wada^{1,*} and Akihisa Inoue²

¹Graduate School, Tohoku University, Sendai 980-8579, Japan

²Institute for Materials Research, Tohoku University, Sendai 980-8577, Japan

Porous Pd_{42.5}Cu₃₀Ni_{7.5}P₂₀ glassy alloy rods with diameters of 7 and 10 mm and a length of about 20 mm were produced by water quenching the mixture of Pd_{42.5}Cu₃₀Ni_{7.5}P₂₀ liquid and solid salt phases at a volume fraction ratio of 7 to 9, followed by leaching treatment into water to eliminate the salt phase. The pores had a polyhedral shape with sizes of 125 to 250 μm. The densities were 3.3 and 4.2 Mg/m³ and their pore fractions were evaluated as 65 and 55% for the 7 mm and 10 mm rods, respectively. The thickness of the cell walls was in the range of 50 to 250 μm. No crystalline phase was observed in the outer surface region as well as in the cell wall region. The glass transition temperature and crystallization temperature of the porous alloy rods were 578 and 679 K, respectively, in agreement with those of the pore-free alloy. Final rupture was not recognized for the porous alloys subjected to the uniaxial compressive test. The porous alloy exhibited lower Young's modulus, lower yield strength, much higher absorption energy, being significantly different from those for the pore-free glassy alloy rod. The unique mechanical characteristics combined with high absorption energy ability indicate the possibility of future uses as a new type of structural and functional materials.

(Received August 4, 2003; Accepted September 1, 2003)

Keywords: bulk glassy alloy, palladium-based alloy, porous materials

1. Introduction

Since glass-type alloys exhibiting glass transition and a large supercooled liquid region prior to crystallization were found in metal-metal alloy systems such as Mg-Ln-(Ni, Cu)^{1,2)} (Ln=lanthanide metal) and Ln-Al-(Ni,Cu)^{3,4)} and Zr-Al-(Ni,Cu)⁵⁾ in the late 1980's, much attention has been paid to the syntheses of new bulk glassy alloys by use of high stability of supercooled liquid against crystallization. For the last one and half decades, a number of bulk glassy alloys have been synthesized in Mg-, Ln-, Zr-, Ti-, Hf-, Fe-, Pd-Cu-, Co-, Ca-, Cu- and Ni-based systems.⁶⁻⁹⁾ The highest glass-forming ability was obtained in the Pd-Cu-Ni-P system¹⁰⁾ and the critical cooling rate for glass formation and the largest sample diameter reached about 0.067 K/s¹¹⁾ and 75 mm,¹²⁾ respectively. When we focus on mechanical strength of bulk glassy alloys, it has been reported that the tensile fracture strength is about 850 MPa¹³⁾ for Mg-based alloys, 1200 MPa¹⁴⁾ for Ln-based alloys, 1500 MPa^{7,9)} for Pd-Cu-based alloys, 1700 MPa¹⁵⁾ for Zr-based alloys, 2100 MPa¹⁶⁾ for Ti-based alloys, 2400 MPa¹⁷⁾ for Cu-based alloys and 2800 MPa¹⁸⁾ for Ni-based alloys. Although these strength values are much higher as compared with conventional crystalline alloys,⁶⁻⁹⁾ the decrease of mass density is expected to cause a further enhancement of engineering value for their bulk glassy alloys. As one of the methods to decrease material density, one can point out the fabrication of porous alloys including high volume fractions of pores. There have been no data on the success of synthesizing bulk glassy alloys containing high volume fractions of pores homogeneously distributed over the whole material. We have recently produced porous bulk glassy Pd-Cu-Ni-P and Pd-Ni-P alloys with the same thermal stability as that for the corresponding pore-free bulk glassy alloys. This paper intends to present the

fabrication, structure, thermal stability and mechanical properties of the porous bulk glassy Pd_{42.5}Cu₃₀Ni_{7.5}P₂₀ alloy.

2. Experimental Procedure

A Pd-based alloy ingot with nominal composition of Pd_{42.5}Cu₃₀Ni_{7.5}P₂₀ was produced by arc melting the mixture of pre-melted Pd-P alloy and pure copper and nickel metals in an argon gas atmosphere. Porous alloy rods with diameters of 7 and 10 mm and a length of 20 mm were produced by water quenching a mixture of the Pd-Cu-Ni-P alloy liquid and solid salt (NaCl) in a silica tube, followed by leaching into water warmed at 353 K to eliminate the salt. The ratio of the Pd-based alloy to NaCl in volume fraction was 7 to 9. The solid salt had a polyhedral shape with sizes ranging from 125 to 250 μm. The pore-free glassy Pd_{42.5}Cu₃₀Ni_{7.5}P₂₀ alloy rod with a diameter of 10 mm was also produced by water quenching the Pd-based alloy liquid in a silica tube. The glassy structure was examined by X-ray diffraction, optical microscopy (OM) and scanning electron microscopy (SEM). Thermal stability associated with glass transition, supercooled liquid region and crystallization were examined by differential scanning calorimetry (DSC) at a heating rate of 0.67 K/s. Mechanical properties in a compressive deformation mode were measured with an Instron testing machine. The aspect ratio of the test specimen was fixed as 2.0. The strain rate was controlled to be $5.0 \times 10^{-4} \text{ s}^{-1}$.

3. Results and Discussion

Figure 1 shows outer shape, transverse and longitudinal cross sections of the Pd_{42.5}Cu₃₀Ni_{7.5}P₂₀ alloy rods with sizes of $\phi 10 \text{ mm} \times 20 \text{ mm}$ and $\phi 7 \text{ mm} \times 20 \text{ mm}$. The transverse and longitudinal cross sectional structures shown in Figs. 1(b) and (c) reveal that the alloy rods contain high volume fractions of pores. No distinct difference in the shape of the

*Graduate Student, Tohoku University.

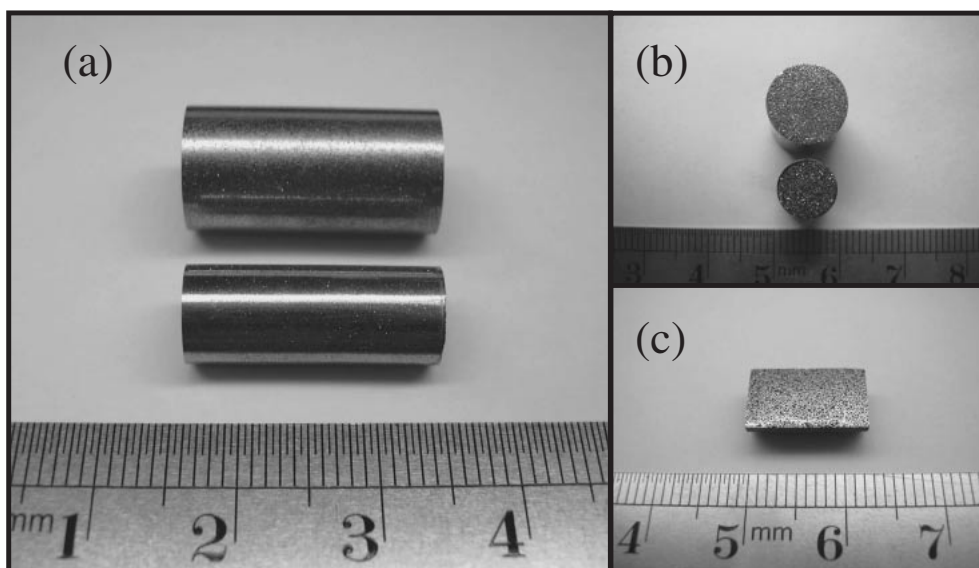


Fig. 1 (a) Outer shape, (b) transverse cross section and (c) longitudinal cross section of the porous $\text{Pd}_{42.5}\text{Cu}_{30}\text{Ni}_{7.5}\text{P}_{20}$ alloy rods with outer dimensions of $\phi 10\text{ mm} \times 20\text{ mm}$ and $\phi 7\text{ mm} \times 20\text{ mm}$ produced by water quenching the mixture of Pd-Cu-Ni-P melt and salt phases at a volume fraction ratio of 7 to 9.

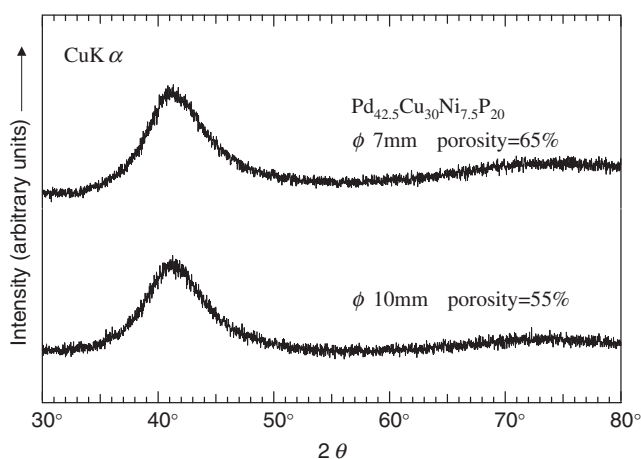


Fig. 2 X-ray diffraction patterns of the porous $\text{Pd}_{42.5}\text{Cu}_{30}\text{Ni}_{7.5}\text{P}_{20}$ alloy rods with diameters of 7 and 10 mm. The porosity was measured as 65 and 55%, respectively.

pores is seen between the two cross sections. The density of the alloy rods was measured to be 4.2 Mg/m^3 for the 10 mm rod and 3.3 Mg/m^3 for the 7 mm rod, and hence the porosity was evaluated to be 55 and 65%, respectively. Figure 2 shows X-ray diffraction patterns of the central region in the transverse cross section of the porous alloy rods. The diffraction patterns consist of broad peaks without any crystalline peaks, indicating that the introduction of high volume fractions of pores does not affect an appreciable harmful influence on the high glass-forming ability.

We also examined the possibility of the reaction between the Pd-Cu-Ni-P liquid and solid salt phases during heating prior to water quenching. In the enlarged SEM image of the surface region of the cell walls (Fig. 3), no additional contrast due to a crystalline phase is observed. The absence of any second phase indicates that the alloy liquid has high resistance against the reaction with the solid salt phase. It is also seen that the pores have a polyhedral shape with sizes

of 125 to 250 μm and the thickness of the cell walls is about 50 to 250 μm . Figure 4 shows DSC curves of the porous Pd-Cu-Ni-P alloy rods with diameters of 7 and 10 mm, together with the data of the pore-free Pd-based alloy rod with a diameter of 10 mm. All the DSC curves have the same features, *i.e.*, the sequent transition of glass transition, followed by a large supercooled liquid region and then crystallization. The glass transition temperature (T_g) and crystallization temperature (T_x) of the porous alloy rods are 578 and 679 K, respectively, in agreement with those of the pore-free alloy rod. It is thus concluded that the thermal stability of the bulk glassy alloys remains unchanged even in the existence of high volume fractions of pores.

Figure 5 shows a nominal stress-strain curve of the porous $\text{Pd}_{42.5}\text{Cu}_{30}\text{Ni}_{7.5}\text{P}_{20}$ alloy rod with a diameter of 10 mm under a uniaxial compressive load, together with the data of the porous-free alloy rod. The feature of the stress-strain curve for the porous alloy rod is significantly different from that of the porous-free alloy rod. It is noticed that final rupture cannot be recognized for the porous alloy up to the nominal strain of 0.9. This is in good contrast to the result that the pore-free glassy alloys instantaneously fracture after a small elastic strain of 0.02. The Young's modulus, yield strength and elastic strain limit are 5.2 GPa, 75 MPa and 0.018, respectively, for the porous alloy and 75 GPa, 1700 MPa and 0.02, respectively, for the pore-free alloy. In addition, the absorption energy up to final failure for the porous alloy was measured to exceed at least 46 MJ/m^3 which is much larger than that (15 MJ/m^3) for the pore-free alloy. Thus, the porous alloy rod has lower Young's modulus, lower yield strength and much larger absorption energy for final rupture as compared with those of the pore-free alloy rod. The significant difference in the mechanical properties is presumably due to the unique polyhedral cellular structure in the porous alloys. The cell walls with smaller cross sections are deformed elastically and plastically at a much lower applied load level. On the other hand, the much larger strain is

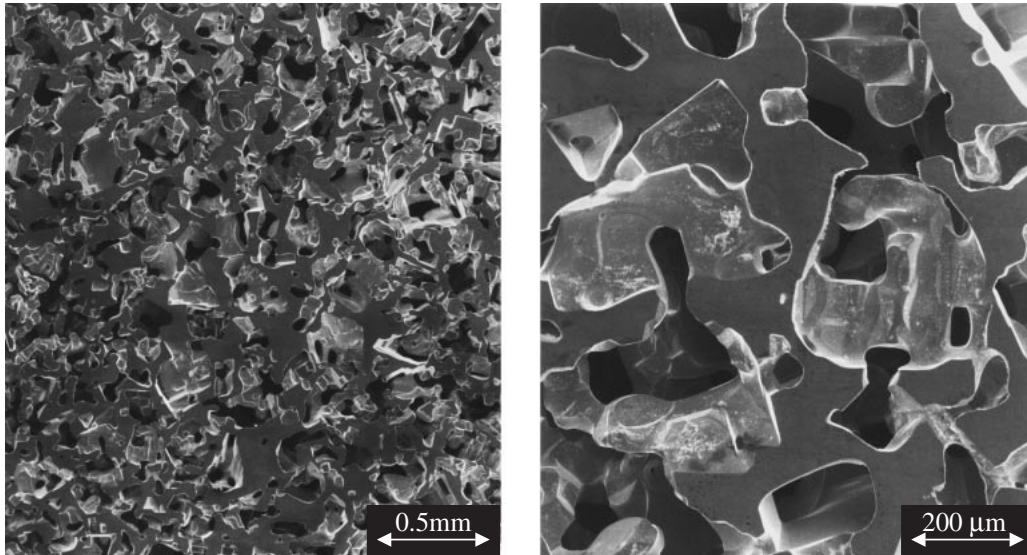


Fig. 3 SEM image revealing the cellular structure in the transverse cross section of the porous glassy Pd_{42.5}Cu₃₀Ni_{7.5}P₂₀ alloy rod with a porosity of 65%.

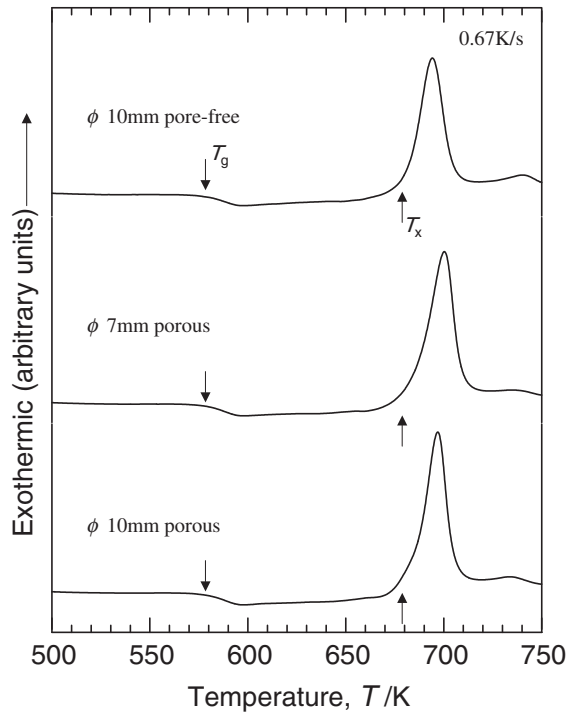


Fig. 4 DSC curves of the porous glassy Pd_{42.5}Cu₃₀Ni_{7.5}P₂₀ alloy rods with diameters of 7 and 10 mm. The data of the pore-free glassy alloy rod with a diameter of 10 mm are also shown for comparison.

presumably because the polyhedral cell walls with different cross sectional areas and various directions to the applied load axis are suffered to multiple stress conditions even under a uniaxial compressive applied load. The enhancement of the plastic deformability of amorphous alloys at room temperature under the multiple stress condition has been demonstrated in the cold drawing treatment of amorphous alloy wires. Such unique mechanical properties which are significantly different from those for the pore-free bulk glassy alloy indicate the possibility of future applications as a new type of structural and functional materials.

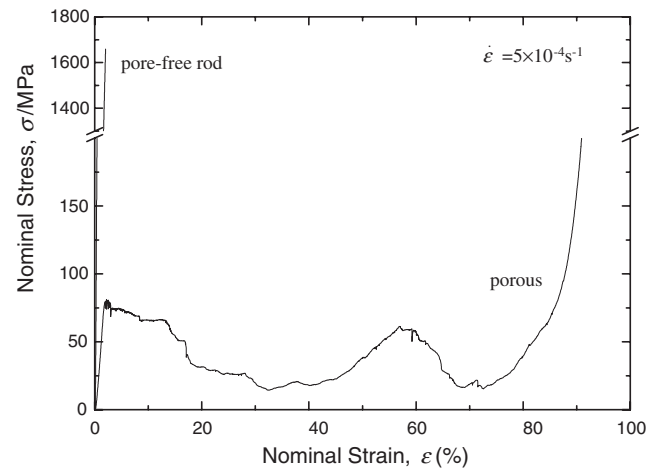


Fig. 5 Compressive nominal stress-strain curve of the porous glassy Pd_{42.5}Cu₃₀Ni_{7.5}P₂₀ alloy rod with a porosity of 55%. The data of the pore-free Pd-Cu-Ni-P alloy rod are also shown for comparison.

4. Summary

We have tried to fabricate porous bulk glassy Pd-Cu-Ni-P alloy rods by water quenching the mixture of the alloy liquid and solid salt, followed by leaching of the salt phase with water. The results obtained are summarized as follows.

(1) By water quenching the mixture of the Pd-Cu-Ni-P alloy liquid and the salt at a ratio of 7 to 9 in volume fraction, porous bulk glassy alloy rods with diameters of 7 and 10 mm were produced. The pores have a polyhedral shape with sizes of 125 to 250 μm . The thickness of the cell walls is in the range of 50 to 250 μm .

(2) The density was about 3.3 Mg/m^3 for the 7 mm rod and 4.2 Mg/m^3 for the 10 mm rod and their porosities were evaluated as 65 and 55%, respectively.

(3) The T_g and T_x were 578 and 679 K, respectively, for the porous alloy rods. No difference in the endothermic and exothermic reactions due to the glass transition and crystallization, respectively, was recognized between the porous

alloy rods and the pore-free alloy rod of 10 mm in diameter.

(4) The porous alloy rod did not suffer to final fracture under a uniaxial compressive load. The Young's modulus, yield strength, elastic strain limit and total absorption energy up to the strain of 0.9 of the porous alloy rod with a diameter of 10 mm are 5.2 GPa, 75 MPa, 0.018 and 46 MJ/m³, respectively, which are characterized as high energy absorption energy materials. The significant difference in mechanical properties in comparison with those for the pore-free alloy rod is interpreted on the basis of the unique polyhedral cell structure.

REFERENCES

- 1) A. Inoue, K. Ohtera, K. Kita and T. Masumoto: *Jpn. J. Appl. Phys.* **27** (1989) L2258-L2261.
- 2) A. Inoue, K. Kohinata, K. Ohtera, A. P. Tsai and T. Masumoto: *Mater. Trans., JIM* **30** (1989) 378-381.
- 3) A. Inoue, T. Zhang and T. Masumoto: *Mater. Trans., JIM* **31** (1989) 965-972.
- 4) A. Inoue, H. Yamaguchi, T. Zhang and T. Masumoto: *Mater. Trans. JIM* **30** (1989) 104-109.
- 5) A. Inoue, T. Zhang and T. Masumoto: *Mater. Trans., JIM* **31** (1990) 177-183.
- 6) A. Inoue: *Mater. Trans. JIM* **36** (1995) 866-875.
- 7) A. Inoue: *Acta Mater.* **48** (2000) 279-306.
- 8) W. L. Johnson: *MRS Bulletin* **24** (1999) 42-56.
- 9) A. Inoue: *Mater. Sci. Eng.* **A304-306** (2001) 1-10.
- 10) A. Inoue, N. Nishiyama and T. Matsuda: *Mater. Trans., JIM* **37** (1996) 181-184.
- 11) N. Nishiyama and A. Inoue: *Intermetallics* **10** (2002) 1952-1956.
- 12) A. Inoue, N. Nishiyama and H. M. Kimura: *Mater. Trans., JIM* **38** (1997) 179-183.
- 13) A. Inoue, A. Kato, T. Zhang, S. G. Kim and T. Masumoto: *Mater. Trans., JIM* **32** (1991) 609-616.
- 14) A. Inoue, T. Nakamura, T. Sugita, T. Zhang and T. Masumoto: *Mater. Trans., JIM* **34** (1993) 351-358.
- 15) A. Inoue and T. Zhang: *Mater. Trans., JIM* **36** (1995) 1184-1187.
- 16) T. Zhang and A. Inoue: *Mater. Trans., JIM* **39** (1989) 1001-1006.
- 17) A. Inoue, T. Zhang, K. Kurosaka and W. Zhang: *Mater. Trans.* **42** (2001) 1800-1804.
- 18) A. Inoue, W. Zhang and T. Zhang: *Mater. Trans.* **43** (2002) 1952-1956.